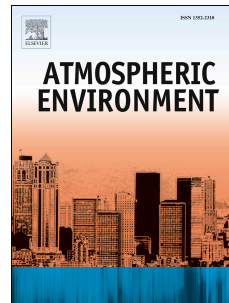


Accepted Manuscript

A method for segregating the optical absorption properties and the mass concentration of winter time urban aerosol

T. Ajtai, N. Utry, M. Pintér, B. Major, Z. Bozóki, G. Szabó



PII: S1352-2310(15)30414-3

DOI: [10.1016/j.atmosenv.2015.09.072](https://doi.org/10.1016/j.atmosenv.2015.09.072)

Reference: AEA 14153

To appear in: *Atmospheric Environment*

Received Date: 4 December 2014

Revised Date: 28 September 2015

Accepted Date: 28 September 2015

Please cite this article as: Ajtai, T., Utry, N., Pintér, M., Major, B., Bozóki, Z., Szabó, G., A method for segregating the optical absorption properties and the mass concentration of winter time urban aerosol, *Atmospheric Environment* (2015), doi: 10.1016/j.atmosenv.2015.09.072.

This is a PDF file of an unedited manuscript that has been accepted for publication. As a service to our customers we are providing this early version of the manuscript. The manuscript will undergo copyediting, typesetting, and review of the resulting proof before it is published in its final form. Please note that during the production process errors may be discovered which could affect the content, and all legal disclaimers that apply to the journal pertain.

1 **A method for segregating the optical absorption properties and**
 2 **the mass concentration of winter time urban aerosol**

3
 4 T. Ajtai^{1,*}, N. Utry², M. Pintér², B. Major², Z. Bozóki¹, G. Szabó¹

5
 6 ¹ Hungarian Academy of Sciences University of Szeged (MTA-SZTE) Research Group on Photoacoustic
 7 Spectroscopy, Dóm tér 9, 6720 Szeged, Hungary

8 ²Department of Optics and Quantum Electronics, University of Szeged, Hungary, Hungarian Academy of
 9 Sciences University of Szeged (MTA-SZTE) Research Group on Photoacoustic Spectroscopy, Dóm tér 9, 6720
 10 Szeged, Hungary

11 *Corresponding author

12 *E-mail address:* ajtai@titan.physx.u-szeged.hu (Tibor Ajtai)

13 **Keywords:** *photoacoustic spectroscopy; aerosol Angström exponent; source apportionment;*
 14 *absorption coefficient; size distribution*

15 **Abstract**

16 A novel in-situ, real time method for the determination of inherent absorption properties of light
 17 absorbing carbonaceous particulate matter and its possible application for source apportionment are
 18 introduced here. The method is deduced from a two-week campaign under wintry urban conditions
 19 during which strong correlation was found between aerosol number size distribution and wavelength
 20 dependent optical absorption coefficient ($AOC(\lambda)$), measured by a Single Mobility Particle Sizer
 21 (SMPS) and a multi-wavelength photoacoustic absorption spectrometer, respectively, while wood
 22 burning and traffic (i.e. fossil fuel burning) activity were identified to be the dominant sources of
 23 carbonaceous particulate. Indeed, during the whole campaign, regardless of the actual emission
 24 strength of the aerosol sources, the measured number size distributions were always dominated by two
 25 unimodal modes with Count Mean Diameter (CMD) of 20 and 100 nm, which could be correlated to
 26 traffic and wood burning activities, respectively. AAE_{ff} , AAE_{wb} (i.e. the Aerosol Angström Exponent of
 27 traffic and wood burning aerosol, respectively), $\sigma_{ff}(266\text{ nm})$, $\sigma_{ff}(1064\text{ nm})$, $\sigma_{wb}(266\text{ nm})$ and $\sigma_{ff}(1064\text{ nm})$ (i.e. the segregated mass specific optical absorption coefficients at two of the measurement
 28 wavelengths) were found to be 1.17 ± 0.18 , 2.6 ± 0.14 , $7.3 \pm 0.3\text{ m}^2\text{g}^{-1}$, $1.7 \pm 0.1\text{ m}^2\text{g}^{-1}$, $3.4 \pm 0.3\text{ m}^2\text{g}^{-1}$ and
 29 $0.31 \pm 0.08\text{ m}^2\text{g}^{-1}$, respectively. Furthermore the introduced methodology can also disentangle and
 30 quantify the temporal variation of both the segregated optical absorptions and the segregated mass
 31 concentrations of traffic and wood burning aerosol. Accordingly, the contribution of wood burning to
 32 optical absorption of PM was found to be negligible at 1064 nm but increased gradually towards the
 33 34 35 36 37 38 39 40 41 42 43 44 45 46 47 48 49 50 51 52 53 54 55 56 57 58 59 60 61 62 63 64 65 66 67 68 69 70 71 72 73 74 75 76 77 78 79 80 81 82 83 84 85 86 87 88 89 90 91 92 93 94 95 96 97 98 99 100 101 102 103 104 105 106 107 108 109 110 111 112 113 114 115 116 117 118 119 120 121 122 123 124 125 126 127 128 129 130 131 132 133 134 135 136 137 138 139 140 141 142 143 144 145 146 147 148 149 150 151 152 153 154 155 156 157 158 159 160 161 162 163 164 165 166 167 168 169 170 171 172 173 174 175 176 177 178 179 180 181 182 183 184 185 186 187 188 189 190 191 192 193 194 195 196 197 198 199 200 201 202 203 204 205 206 207 208 209 210 211 212 213 214 215 216 217 218 219 220 221 222 223 224 225 226 227 228 229 230 231 232 233 234 235 236 237 238 239 240 241 242 243 244 245 246 247 248 249 250 251 252 253 254 255 256 257 258 259 260 261 262 263 264 265 266 267 268 269 270 271 272 273 274 275 276 277 278 279 280 281 282 283 284 285 286 287 288 289 290 291 292 293 294 295 296 297 298 299 300 301 302 303 304 305 306 307 308 309 310 311 312 313 314 315 316 317 318 319 320 321 322 323 324 325 326 327 328 329 330 331 332 333 334 335 336 337 338 339 340 341 342 343 344 345 346 347 348 349 350 351 352 353 354 355 356 357 358 359 360 361 362 363 364 365 366 367 368 369 370 371 372 373 374 375 376 377 378 379 380 381 382 383 384 385 386 387 388 389 390 391 392 393 394 395 396 397 398 399 400 401 402 403 404 405 406 407 408 409 410 411 412 413 414 415 416 417 418 419 420 421 422 423 424 425 426 427 428 429 430 431 432 433 434 435 436 437 438 439 440 441 442 443 444 445 446 447 448 449 450 451 452 453 454 455 456 457 458 459 460 461 462 463 464 465 466 467 468 469 470 471 472 473 474 475 476 477 478 479 480 481 482 483 484 485 486 487 488 489 490 491 492 493 494 495 496 497 498 499 500 501 502 503 504 505 506 507 508 509 510 511 512 513 514 515 516 517 518 519 520 521 522 523 524 525 526 527 528 529 530 531 532 533 534 535 536 537 538 539 540 541 542 543 544 545 546 547 548 549 550 551 552 553 554 555 556 557 558 559 560 561 562 563 564 565 566 567 568 569 570 571 572 573 574 575 576 577 578 579 580 581 582 583 584 585 586 587 588 589 590 591 592 593 594 595 596 597 598 599 600 601 602 603 604 605 606 607 608 609 610 611 612 613 614 615 616 617 618 619 620 621 622 623 624 625 626 627 628 629 630 631 632 633 634 635 636 637 638 639 640 641 642 643 644 645 646 647 648 649 650 651 652 653 654 655 656 657 658 659 660 661 662 663 664 665 666 667 668 669 670 671 672 673 674 675 676 677 678 679 680 681 682 683 684 685 686 687 688 689 690 691 692 693 694 695 696 697 698 699 700 701 702 703 704 705 706 707 708 709 710 711 712 713 714 715 716 717 718 719 720 721 722 723 724 725 726 727 728 729 730 731 732 733 734 735 736 737 738 739 740 741 742 743 744 745 746 747 748 749 750 751 752 753 754 755 756 757 758 759 750 751 752 753 754 755 756 757 758 759 760 761 762 763 764 765 766 767 768 769 770 771 772 773 774 775 776 777 778 779 770 771 772 773 774 775 776 777 778 779 780 781 782 783 784 785 786 787 788 789 780 781 782 783 784 785 786 787 788 789 790 791 792 793 794 795 796 797 798 799 790 791 792 793 794 795 796 797 798 799 800 801 802 803 804 805 806 807 808 809 800 801 802 803 804 805 806 807 808 809 810 811 812 813 814 815 816 817 818 819 810 811 812 813 814 815 816 817 818 819 820 821 822 823 824 825 826 827 828 829 820 821 822 823 824 825 826 827 828 829 830 831 832 833 834 835 836 837 838 839 830 831 832 833 834 835 836 837 838 839 840 841 842 843 844 845 846 847 848 849 840 841 842 843 844 845 846 847 848 849 850 851 852 853 854 855 856 857 858 859 850 851 852 853 854 855 856 857 858 859 860 861 862 863 864 865 866 867 868 869 860 861 862 863 864 865 866 867 868 869 870 871 872 873 874 875 876 877 878 879 870 871 872 873 874 875 876 877 878 879 880 881 882 883 884 885 886 887 888 889 880 881 882 883 884 885 886 887 888 889 890 891 892 893 894 895 896 897 898 899 890 891 892 893 894 895 896 897 898 899 900 901 902 903 904 905 906 907 908 909 900 901 902 903 904 905 906 907 908 909 910 911 912 913 914 915 916 917 918 919 910 911 912 913 914 915 916 917 918 919 920 921 922 923 924 925 926 927 928 929 920 921 922 923 924 925 926 927 928 929 930 931 932 933 934 935 936 937 938 939 930 931 932 933 934 935 936 937 938 939 940 941 942 943 944 945 946 947 948 949 940 941 942 943 944 945 946 947 948 949 950 951 952 953 954 955 956 957 958 959 950 951 952 953 954 955 956 957 958 959 960 961 962 963 964 965 966 967 968 969 960 961 962 963 964 965 966 967 968 969 970 971 972 973 974 975 976 977 978 979 970 971 972 973 974 975 976 977 978 979 980 981 982 983 984 985 986 987 988 989 980 981 982 983 984 985 986 987 988 989 990 991 992 993 994 995 996 997 998 999 990 991 992 993 994 995 996 997 998 999 1000 1001 1002 1003 1004 1005 1006 1007 1008 1009 1000 1001 1002 1003 1004 1005 1006 1007 1008 1009 1010 1011 1012 1013 1014 1015 1016 1017 1018 1019 1010 1011 1012 1013 1014 1015 1016 1017 1018 1019 1020 1021 1022 1023 1024 1025 1026 1027 1028 1029 1020 1021 1022 1023 1024 1025 1026 1027 1028 1029 1030 1031 1032 1033 1034 1035 1036 1037 1038 1039 1030 1031 1032 1033 1034 1035 1036 1037 1038 1039 1040 1041 1042 1043 1044 1045 1046 1047 1048 1049 1040 1041 1042 1043 1044 1045 1046 1047 1048 1049 1050 1051 1052 1053 1054 1055 1056 1057 1058 1059 1050 1051 1052 1053 1054 1055 1056 1057 1058 1059 1060 1061 1062 1063 1064 1065 1066 1067 1068 1069 1060 1061 1062 1063 1064 1065 1066 1067 1068 1069 1070 1071 1072 1073 1074 1075 1076 1077 1078 1079 1070 1071 1072 1073 1074 1075 1076 1077 1078 1079 1080 1081 1082 1083 1084 1085 1086 1087 1088 1089 1080 1081 1082 1083 1084 1085 1086 1087 1088 1089 1090 1091 1092 1093 1094 1095 1096 1097 1098 1099 1090 1091 1092 1093 1094 1095 1096 1097 1098 1099 1100 1101 1102 1103 1104 1105 1106 1107 1108 1109 1110 1111 1112 1113 1114 1115 1116 1117 1118 1119 1110 1111 1112 1113 1114 1115 1116 1117 1118 1119 1120 1121 1122 1123 1124 1125 1126 1127 1128 1129 1130 1131 1132 1133 1134 1135 1136 1137 1138 1139 1130 1131 1132 1133 1134 1135 1136 1137 1138 1139 1140 1141 1142 1143 1144 1145 1146 1147 1148 1149 1140 1141 1142 1143 1144 1145 1146 1147 1148 1149 1150 1151 1152 1153 1154 1155 1156 1157 1158 1159 1150 1151 1152 1153 1154 1155 1156 1157 1158 1159 1160 1161 1162 1163 1164 1165 1166 1167 1168 1169 1160 1161 1162 1163 1164 1165 1166 1167 1168 1169 1170 1171 1172 1173 1174 1175 1176 1177 1178 1179 1170 1171 1172 1173 1174 1175 1176 1177 1178 1179 1180 1181 1182 1183 1184 1185 1186 1187 1188 1189 1180 1181 1182 1183 1184 1185 1186 1187 1188 1189 1190 1191 1192 1193 1194 1195 1196 1197 1198 119

36 shorter wavelengths and became commensurable with the optical absorption of traffic at 266 nm
37 during the whole measurement period. Furthermore, the contribution of wood burning mass to CM
38 (mass of carbonaceous particulate matter) was dominant regardless of the strength of the emission
39 activity of traffic and wood burning during the whole measurement period.

40

41 **1. Introduction**

42 The investigation of light absorbing carbonaceous particulate matter (LAC) is of utmost
 43 importance in the fields of atmospheric physics and chemistry. LAC is one of the most prominent
 44 drivers of global warming, while the uncertainties associated with radiative forcing calculations are
 45 also dominantly linked to its components (Penner et al., 2001; Schwartz, 2004; Lack et al., 2006;
 46 Solomon et al., 2007; Bond et al., 2013). On a regional scale, LAC is a major concern as an air
 47 pollutant, especially considering its adverse health effects and the public debate concerning its legal
 48 regulation.

49 It has been experimentally demonstrated in many recent studies, that LAC is dominantly
 50 composed of traffic and wood burning aerosol particularly under wintertime urban conditions, when
 51 the biological and photochemical activities are negligible (Sandradewi et al., 2008a, b; Favez et al.,
 52 2009). So far public policies have been committed to reducing the emission caused by traffic, industry
 53 and power plants while wood burning has been regarded as a renewable energy source with CO₂
 54 neutral emission as an alternative for residential heating. Therefore, the relative amount of the wood
 55 burning aerosol fraction is expected to increase in the total mass of PM at an accelerating rate in the
 56 future.

57 Several methods have been introduced to quantitatively apportion aerosol fractions emitted by
 58 wood burning and traffic but most of them require time consuming and costly off-line chemical
 59 analysis. The recently developed semi continuous EC/OC ratio measurement based on the thermo-
 60 optical method using NIOSH 5040 protocol (Chow et al., 2001) or the real-time composition
 61 identification carried out by the aerosol mass spectrometer (AMS) are now also available for on-line
 62 source apportionment and open up novel possibilities in this field (Lanz et al., 2007; Kleinman et al.,
 63 2002). However, although they are extremely powerful tools for source apportionment, their
 64 widespread and regular application is limited mainly by instrument prices and laboratory costs.

65 As opposed to chemical features, the microphysical properties of airborne particles such as
 66 optical absorption, light scattering, and size distribution can be easily measured on-line, with high
 67 accuracy and sensitivity, especially under highly polluted urban conditions (Wehner and
 68 Wiedensohler, 2003; Kleinman et al., 2002; Scaire et al., 2008). Unfortunately in most of the cases
 69 there is a limited possibility of deducing chemical information from the measured microphysical data
 70 as most of them are not unique indicators of chemical composition (Utry et al., 2014). Nevertheless,
 71 some recent laboratory and field studies have demonstrated that although the optical absorption
 72 coefficient in itself does not, its wavelength dependency could correlate with chemical composition
 73 (Favez et al., 2009, 2010; Lewis et al., 2008; Chakrabatry et al., 2010; Flowers et al., 2010; Ajtai et al.,
 74 2011b). Therefore, the multi-wavelength measurement of optical absorption could yield a chemically

75 selective parameter in a real time source apportionment model (Moosmüller et al., 2011; Sandradewi
 76 et al., 2008a, b; Favez et al., 2010; Ajtai et al., 2011b).

77 Sandradewi et al. (2008) have been the first to propose a new method for the apportionment of
 78 wood burning and traffic aerosols based on the real time measurement of the multi-wavelength
 79 absorption spectra. Since all the early applications of this method have been based on transmission
 80 measurement on filter accumulated aerosol using a multi-wavelength Aethalometer, it is commonly
 81 called as the “Aethalometer model” in the literature. Although in some very recent studies both the
 82 applied method used for absorption measurement and the model itself have been criticized (Harrison et
 83 al., 2013), due to its simplicity and effectiveness this approach is likely to become more and more
 84 widely used. The original “Aethalometer model” is based on supplementary measurements of the
 85 chemical properties of the aerosol via filter sampling and off-line chemical analysis. However, due to
 86 the inherent problems associated with filter measurements, such as the limited sensitivity (which
 87 necessitates long time sampling) and the limited reliability of data interpretations (due to sampling and
 88 methodology artefact) as well as their off-line nature (Andreae and Gelencsér, 2006; Moosmüller et
 89 al., 2009; Schnaiter et al., 2005), various assumptions and simplifications are introduced into the
 90 Aethalometer model, which however further decrease its reliability.

91 In the present study we propose a novel type of source apportionment methodology based on
 92 in-situ, filter-free characterization of the ambient carbon fraction by simultaneous measurement of
 93 aerosol light absorption and size distribution using our state-of-the-art multi-wavelength photoacoustic
 94 spectrometer (4λ-PAS) and a Single Mobility Particle Sizer (SMPS), respectively. Measurements were
 95 carried out under wintertime ambient conditions, during which the sources of carbonaceous particulate
 96 matter were found to be traffic and wood burning practically exclusively.

97

98 **2. Sampling site and instrumentation**

99 *2.1. Measurement site*

100 The measurements reported here were carried out under wintertime urban ambient conditions
 101 near the city center of Szeged, Hungary (46.26°N, 20.14°E), from 12 to 26 of January, 2011. Szeged is
 102 among of the most populated cities of Hungary with more than 170000 inhabitants. According to the
 103 Hungarian Central Statistical Office (KSH) Szeged has the highest ratio of individual to district
 104 heating throughout the country, which is dominated by wood burning (Utry et al., 2013). Furthermore,
 105 during the campaign period, the city was also suffering from extremely high traffic activity, i.e. over
 106 3000 trucks were passing through the city center daily, right next to the monitoring station. As a result
 107 of the high concentrations of typical wintertime urban carbonaceous particulate matter (traffic and
 108 residential heating aerosol) and the periodically varying ratio of these carbon constituents, this

109 measurement site was ideal to study the optical responses of typical wintertime urban ambience under
 110 continuously changing emission strengths of traffic and wood burning (Utry et al., 2013)

111

112 *2.2. Instrumentations and sampling.*

113 The absorption response of the ambient atmosphere was measured by our recently developed
 114 state-of-the-art multi-wavelength photoacoustic spectrometer (4 λ -PAS). The filter free operation and
 115 the insensitivity to scattering, as well as the wide range of operational wavelengths from near-IR to
 116 UV provides absorption data with high reliability (Flowers et al., 2010; Utry et al., 2014). The
 117 principles of operation and the characteristic performance of this instrument both under laboratory and
 118 field conditions are described in details elsewhere (Ajtai et al., 2010; 2011). The aerosol optical
 119 absorption coefficient (AOC) was determined at all operational wavelengths of the 4 λ -PAS (266nm,
 120 355nm, 532nm and 1064nm). The accuracy of this instrument was proved to be below 2-6% depending
 121 on the applied wavelengths due to the implemented wavelength independent gas-phase calibration
 122 (Ajtai et al., 2010).

123 Number and volume concentration as well as the size distribution of the atmospheric aerosol
 124 were measured by the Scanning Mobility Particle Sizer (SMPS, GRIMM system Aerosol Technik,
 125 Germany, type SMPS+C) and by the Optical Particle Counter (OPC, GRIMM, Aerosol Technik,
 126 Germany, type 1.108), respectively in the size range from 5 nm to 32 μm . SMPS consists of the
 127 Condensation Particle Counter (CPC Model #5.400) and the Classifier “Vienna”-Type Differential
 128 Mobility Analyzer (DMA, Model #5.500). The “short” DMA was used to measure the fine fraction of
 129 ambient particulate matter from 5 nm to 350 nm. First, the DMA separates particles in the equally
 130 charged aerosol stream according to their electrical mobility. Following that the separated particles are
 131 lead to the CPC unit where the size-segregated number density is measured. The shielding effect,
 132 which occurs when high concentrations of particles get into the DMA, is minimized by using the
 133 shelf-implemented coincidence correction protocol. The Optical Particle Counter (OPC, GRIMM
 134 Aerosol Technic, Germany, type 1.108) was used to measure the size distribution in the coarse fraction
 135 from 0.3nm to 32 μm size range according to the light scattering intensity of the aerosol stream.

136

137 **3. The apportionment method**

138 *3.1. The assumptions behind the extrapolation method*

139 The applicability of the above described extrapolation method (and the validity of Equation 3-
 140 6) depends on whether the following assumptions are fulfilled throughout the studied measurement
 141 period, independently of the actual intensity of the traffic and wood burning sources:

- Optical absorption coefficient ($AOC(\lambda)$) can be written as the sum of the optical absorption coefficient of wood burning aerosol ($AOC_{ff}(\lambda)$) and the optical absorption coefficient of traffic aerosol ($AOC_{wb}(\lambda)$) at any of the used measurement wavelengths (see Equation 3 and 4).
- Both the traffic and the wood burning aerosol fraction can be characterized with a well distinguishable characteristic unimodal mode in the number size distribution and the concentration of light absorbing carbonaceous aerosol can be written with a good accuracy as the sum of wood burning (N_{wb}) and traffic (N_{ff}) aerosol number concentration within these characteristic modes. This and the previous assumption state the dominance of these two aerosol types in the light absorbing fraction of the atmospheric aerosol.
- The wood burning and the traffic aerosol can be characterized unambiguously by single particle optical absorption coefficients ($SPAOC_{wb}(\lambda)$ and ($SPAOC_{ff}(\lambda)$, respectively) at any of the used measurement wavelengths. The applicability of Equation 5 and 6 depends on this and the previous assumptions.

The first two assumptions will be discussed in details in 3.2.1. The presented results prove that the third assumption is valid at least during the period of this relatively short campaign. Its long term validity will be a subject of further field campaigns.

159

160 3.2. The extrapolation method for the determination of the segregated AAEs

161 The introduced method consists of four subsequent steps (see below) and it is based on the
162 following Equations:

$$163 \frac{AOC_{ff}(\lambda_1)}{AOC_{ff}(\lambda_2)} = \left[\frac{\lambda_1}{\lambda_2} \right]^{-AAE_{ff}} \quad (1)$$

$$164 \frac{AOC_{wb}(\lambda_1)}{AOC_{wb}(\lambda_2)} = \left[\frac{\lambda_1}{\lambda_2} \right]^{-AAE_{wb}} \quad (2)$$

$$165 AOC(\lambda_1) = AOC_{ff}(\lambda_1) + AOC_{wb}(\lambda_1) \quad (3)$$

$$166 AOC(\lambda_2) = AOC_{ff}(\lambda_2) + AOC_{wb}(\lambda_2) \quad (4)$$

$$167 AOC(\lambda_1) = N_{ff} \times SPAOC_{ff}(\lambda_1) + N_{wb} \times SPAOC_{wb}(\lambda_1) \quad (5)$$

$$168 AOC(\lambda_2) = N_{ff} \times SPAOC_{ff}(\lambda_2) + N_{wb} \times SPAOC_{wb}(\lambda_2) \quad (6)$$

$$169 CM(PM_1) = \sigma_{ff}(\lambda_1)^{-1} \times AOC_{ff}(\lambda_1) + \sigma_{wb}(\lambda_1)^{-1} \times AOC_{wb}(\lambda_1) \quad (7)$$

170 $CM(PM_1) = \sigma_{ff}(\lambda_2)^{-1} \times AOC_{ff}(\lambda_2) + \sigma_{wb}(\lambda_2)^{-1} \times AOC_{wb}(\lambda_2)$ (8)

171 $CM_{wb}(PM1) = AOC_{wb}(\lambda) \times \sigma_{wb}(\lambda)$

172 (9)

173 $CM_{ff}(PM1) = AOC_{ff}(\lambda) \times \sigma_{ff}(\lambda)$

174 (10),

175 where λ is wavelength, $AOC_{ff}(\lambda)$ and $AOC_{wb}(\lambda)$ are the optical absorption coefficient of fossil fuel
 176 and wood burning aerosol at the given wavelength, $AOC(\lambda)$ is optical absorption coefficient measured
 177 at the given wavelength, N_{ff} and N_{wb} are total number concentration of fossil fuel and wood burning
 178 aerosol, $SPAOC_{ff}(\lambda)$ and $SPAOC_{wb}(\lambda)$ are single particle optical absorption coefficient of fossil fuel
 179 and wood burning aerosol at the given wavelength, $CM(PM_1)$ is mass concentration of carbonaceous
 180 particulate matter, PM1, $\sigma_{ff}(\lambda)$ and $\sigma_{wb}(\lambda)$ are mass specific optical absorption coefficient of fossil
 181 fuel and wood burning aerosol at the given wavelength, while $CM_{ff}(PM1)$ and $CM_{wb}(PM1)$ is mass
 182 concentration of fossil fuel and wood burning aerosol respectively.

183 1. As a first step the segregated Absorption Angstrom Exponents (defined by Eq. 1 and 2) of
 184 traffic and wood burning aerosol (AAE_{ff} and AAE_{wb} , respectively) is determined with the help
 185 of an extrapolation method which is based on Eq. 3-6 and described in details in this section.
 186 The applicability of the extrapolation method depends on the validity of a few assumptions
 187 listed in this section which are verified in 3.2.1.

188 2. In the next step the temporal variations of the segregated aerosol optical absorption
 189 coefficients (AOC) for traffic and wood burning components ($AOC_{ff}(\lambda)$ and $AOC_{wb}(\lambda)$,
 190 respectively) throughout the campaign are calculated with the help of Eq. 1-4. Indeed once the
 191 AAE values are known from the previous step, these four equations only contain four
 192 unknown quantities, i.e. for each measurement point they can be solved algebraically.

193 3. Segregated mass specific optical absorption coefficients of traffic and wood burning aerosol
 194 ($\sigma_{ff}(\lambda)$ and $\sigma_{wb}(\lambda)$, respectively) is determined with the help of Eq. 7 and 8, where
 195 $CM(PM_1)$ means the mass concentration of sub-micron sized carbonaceous particulate matter
 196 measured by an independent method. See section 3.3 for details.

197 4. Finally by dividing the segregated AOC values with the corresponding σ values the temporal
 198 variation of the segregated mass concentrations can be determined as given in Eq. 9 and 10.

199 The ultimate operational wavelengths (266 and 1064 nm) were selected here to demonstrate the
 200 applicability of the introduced method, because the contribution of the traffic and wood burning
 201 aerosol particles to the optical absorption was expected to be the most divers at these wavelengths,
 202 resulting in higher apportionment selectivity. By writing the two actual measurement wavelengths

203 (266 nm and 1064 nm) into Eq. 5 and Eq. 6, respectively and dividing Eq. 5 by Eq. 6, one gets the
 204 following equation:

$$205 \quad \frac{AOC(266nm)}{AOC(1064nm)} = \frac{SPAOC_{ff}(266nm) + \frac{N_{100}}{N_{20}} \cdot SPAOC_{wb}(266nm)}{SPAOC_{ff}(1064nm) + \frac{N_{100}}{N_{20}} \cdot SPAOC_{wb}(1064nm)} \quad (9)$$

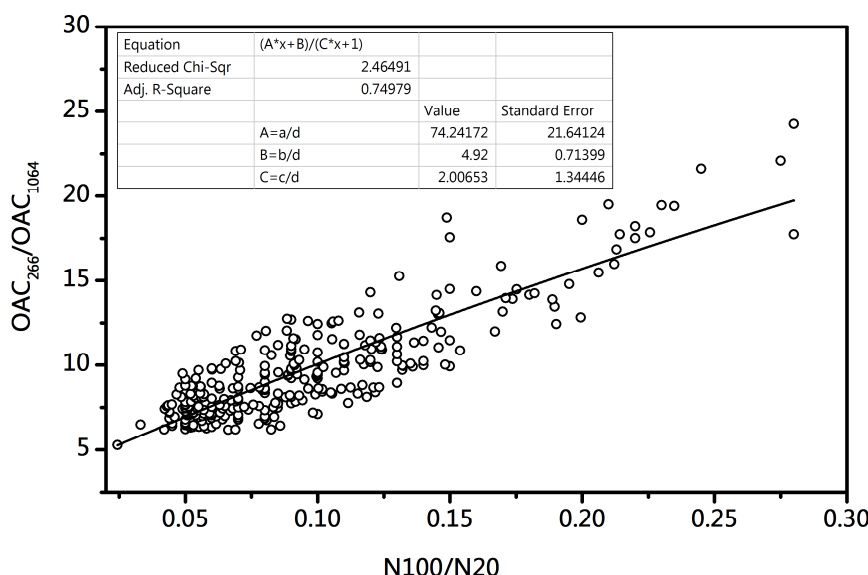
206 N_{100} and N_{20} stands for the number concentration of particle associated to the identified modes
 207 with count median diameter of 100 nm and 20 nm, respectively.

208 Figure 1 shows the ratio of the measured AOCs as a function of N_{100}/N_{20} . In case N_{100}/N_{20}
 209 converges to either 0 or infinity, Eq. 9 can be rewritten as:

$$210 \quad \lim_{\frac{N_{100}}{N_{20}} \rightarrow 0} \frac{AOC(266nm)}{AOC(1064nm)} = \frac{SPAOC_{wb}(266nm)}{SPAOC_{wb}(1064nm)} = \left(\frac{266}{1064} \right)^{-AAE_{ff}} \quad (10)$$

$$211 \quad \lim_{\frac{N_{100}}{N_{20}} \rightarrow \infty} \frac{AOC(266nm)}{AOC(1064nm)} = \frac{SPAOC_{ff}(266nm)}{SPAOC_{ff}(1064nm)} = \left(\frac{266}{1064} \right)^{-AAE_{wb}} \quad (11)$$

212 i.e. in these limits, which correspond to cases when the light absorption is totally dominated either by
 213 traffic or wood burning aerosol, respectively, the segregated AAE values can be determined. The
 214 segregated AAE values can be determined by fitting data points shown on Figure 1 the function shown
 215 on Fig. 1. and calculating the asymptotic value of the fitted curve (see section 4 for results).

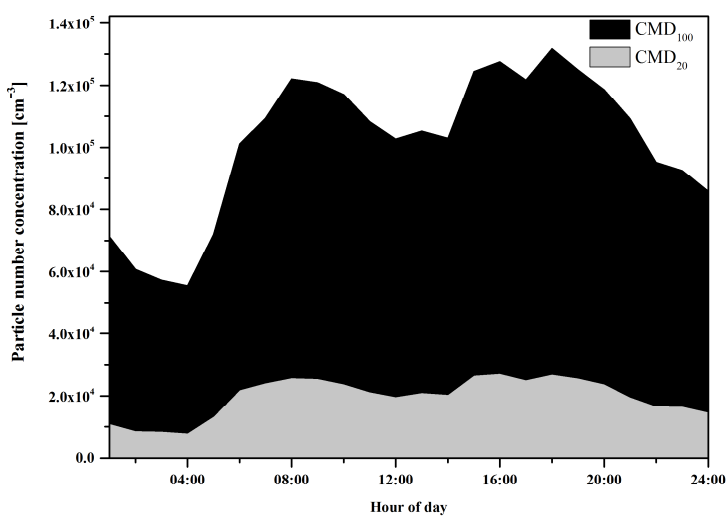


216

217 *Figure 1. Measured optical absorption coefficient ratios as a function of the ratio of the number
 218 concentrations in the two aerosol modes (see text for details)*

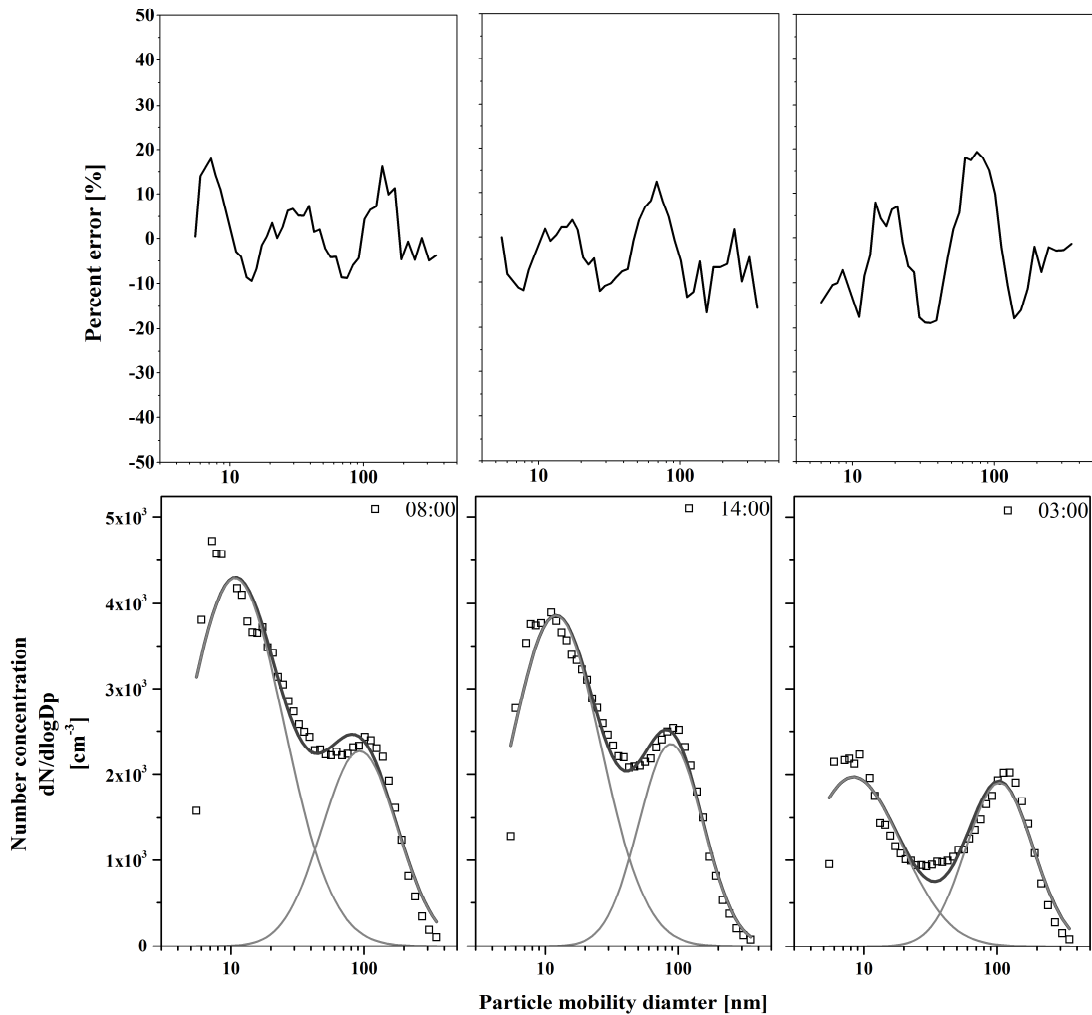
219 *3.2.1. Segregated number size distributions*

220 Throughout the reported measurement campaign two characteristic mode with a Count Median
 221 Diameter of 20 nm (CMD_{20}) and 100 nm (CMD_{100}), respectively could always be identified in the
 222 measured number size distributions. Their relative weight varied in time but nevertheless almost all
 223 measured particles were found to belong to either mode. In our previous study (Utry et al., 2014) the
 224 CMD_{20} and CMD_{100} modes were attributed to traffic and residential wood burning for household
 225 heating, respectively. This assignment is justified both by the results of off-line chemical analysis and
 226 by the daily variation of the ratio of segregated number size concentrations in the CMD_{100} and CMD_{20}
 227 modes (i.e. N_{ff}/N_{wb}) which reached its maximum at 18:00 and at around 8:00 (i.e. during rush hours),
 228 while having a local and an absolute minima at around 12:00 and 3:00, respectively. The average daily
 229 variation (taking into account only working days, i.e. excluding week-ends) of N_{ff} and N_{wb} are shown
 230 in Figure 2. Furthermore, we also found that the two modes add up to the original size distribution
 231 during any period of the day with good accuracy (Figure 3). These findings are in line with the widely
 232 adopted assumption that under typical wintry urban conditions whenever individual heating (i.e. wood
 233 burning) dominates, the fine fraction of ambient aerosol (<PM1) does almost exclusively include
 234 carbonaceous particulate matter from traffic (CMD_{20}) and from residential heating (CMD_{100})
 235 (Schneider et al., 2005; Bond et al., 2002; Wehner and Wiedensohler, 2003; Rissle et al., 2006). Based
 236 on the presented results the validity of Eq. 5 and 6 can be indeed assumed. However it should be noted
 237 that the separation of the size distribution into two modes is possible only if number representation is
 238 used while e.g. the volumetric representation cannot be applied as explained elsewhere (Schneider et
 239 al., 2005; Hedberg et al., 2002).



240

241 *Figure 2. The daily variation of the segregated number-concentration in the $CMD=20\text{nm}$ and*
 242 *$CMD=100\text{nm}$ modes.*



243

244 *Figure 3. The lower panel contains the segregated (unimodal) number-size distributions (grey lines),*
 245 *the sum of these modes (black lines) and the originally measured number size distributions (dots) at*
 246 *three characteristic time of the day. The upper panel contains the percent errors between the*
 247 *measured and the calculated (from the segregated) number size distributions.*

248

249 3.3 The determination of the segregated mass specific optical absorption coefficients

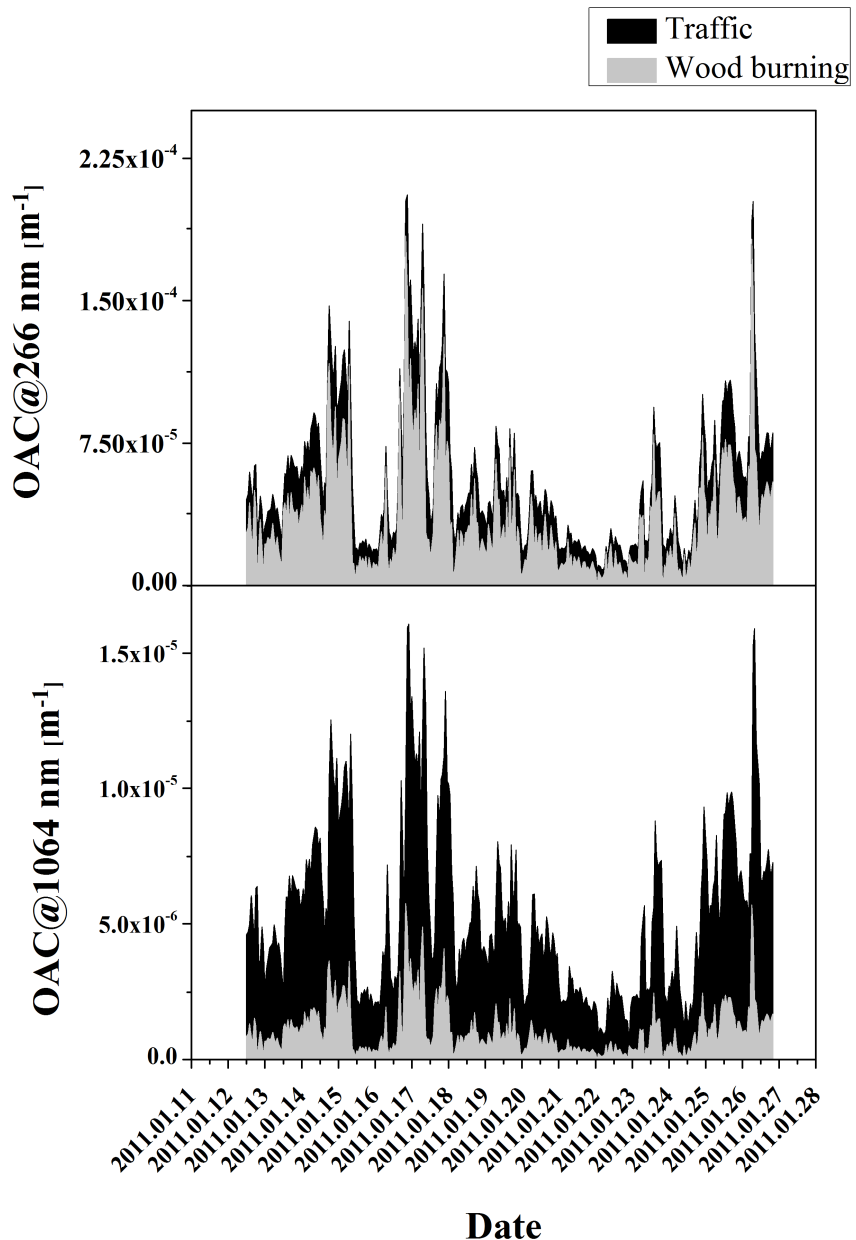
250 The extrapolation method discussed above yields valuable information on the segregated
 251 optical properties of the aerosol ambience. The segregated mass concentrations can also be calculated
 252 by using Eq. 7 and 8 and the measured AOC values whenever the temporal variation of the total mass
 253 concentration in the PM1 mode (CM(PM1)) is available. In case of the measurement campaign
 254 analyzed in this publication, the mass concentration was calculated from the volume-concentration
 255 measured by the SMPS assuming an average carbonaceous particle density of $1.5\mu\text{g}/\text{m}^3$ which is one
 256 of the most cited and accepted average values of ambient carbonaceous particulate in the literature
 257 (McCurry et al., 2010; Turpin and Lim, 2001). Unfortunately as the particle density of traffic and
 258 wood burning aerosol varies in a wide range between $1.3\text{-}2.2\mu\text{g}/\text{m}^3$ and depends on the operation

259 conditions of combustion as well as the type of fuel (Burtscher 2004; Park et al., 2004; Dinar et al.,
260 2006), one can question the reliability of the calculated segregated mass concentrations. On the other
261 hand in future applications of the apportionment method one can always use e.g. a TEOM or a beta
262 attenuation monitor possibly combined with a PM1 impactor for the independent determination of
263 CM(PM1) so this limitation should not apply in general.

264

265 **4. Results**

266 By using the extrapolation method described in details in section 3.2.1, AAE_{ff} and AAE_{wb} found
267 to be 1.17 ± 0.18 and 2.6 ± 0.14 , respectively. The correlation coefficient and the standard deviation of
268 the fitting were found to be 0.74 and 0.05 respectively. The time series of one hour averaged data of
269 AOC_{ff} and AOC_{wb} determined at 266 and 1064nm wavelengths are plotted in Figure 4. The mass
270 specific absorption coefficient of traffic and wood burning aerosol was calculated to be $\sigma_{ff}(266\text{nm}) =$
271 $7.3 \pm 0.4 \text{ m}^2/\text{g}$, $\sigma_{ff}(1064\text{nm}) = 1.7 \pm 0.23 \text{ m}^2/\text{g}$ and $\sigma_{wb}(266\text{nm}) = 3.4 \pm 0.18 \text{ m}^2/\text{g}$, and $\sigma_{wb}(1064\text{nm}) =$
272 $0.31 \pm 0.1 \text{ m}^2/\text{g}$ using Eq. 7 and 8. The calculated temporal variation of the mass concentration of
273 traffic and wood burning aerosol are plotted in Fig.5.

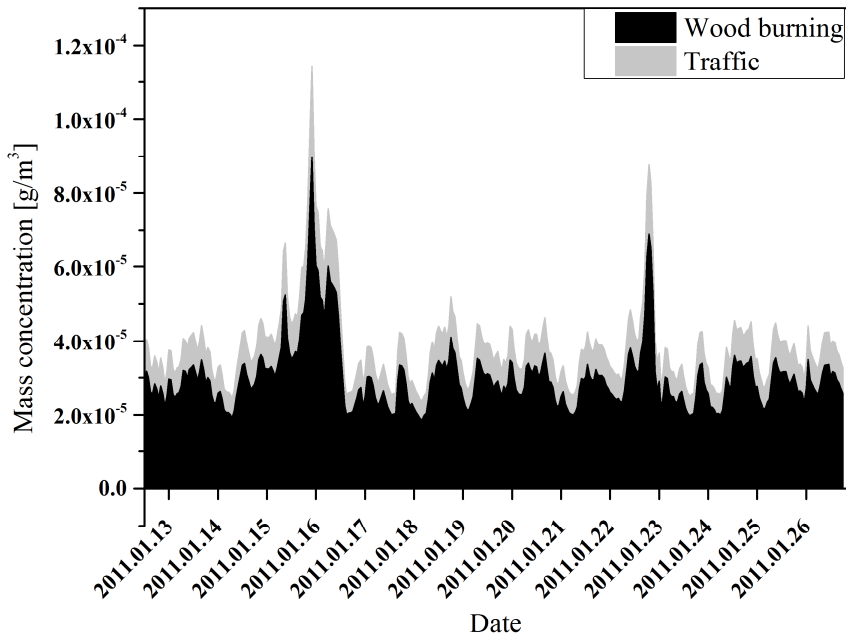


274

275
276

Figure 4. Temporal variation of the segregated AOC values at the two wavelengths of the 4 λ -PAS instrument

277



278

279 *Figure. 5. Segregated mass concentration of wood burning and traffic aerosol determined by the*
 280 *introduced method*

281

282 **5. Discussion**

283 The correlation coefficients and the standard deviation of the fitting parameters of the
 284 extrapolation method for the determination of the segregated AAE values indicate strong and reliable
 285 relationship between the measured parameters. The deduced AAE_{ff} value is very similar to both
 286 theoretical predictions (AAE_{ff} is expected to be approximately 1) from the literature which are based on
 287 the corpuscular approximation and also with results from other experiments made both under
 288 laboratory and field conditions (Lan et al., 2013; Russel et al., 2013; Favez et al., 2009). The
 289 calculated AAE_{wb} value is also analogous with AAE_{wb} values determined during other field studies
 290 (Sandradewi et al., 2008b; Lewis et al., 2008; Moosmüller et al., 2011). Indeed AAE_{wb} is known to
 291 vary in a wide range from 1.3 up to around 3 while it also depends on the type of wood and the
 292 condition of combustion (Bond, 2001; Kirchstetter et al., 2004; Schnaiter et al., 2003).

293 In the extrapolation method only two out of the four available wavelengths of the 4λ -PAS
 294 instrument is used. Indeed it can be seen (Fig. 4) that the temporally varying AOC is dominated by
 295 AOC_{ff} and AAE_{wb} in the near-infrared and in the UV, respectively. These findings can be well
 296 explained by the inherent optical properties of these aerosols, since wood smoke is likely to contain
 297 high abundant organic compositions such as HULIS (Humic-Like Substances), PAH (Polycyclic
 298 Aromatic Hydrocarbons) which has gradually increasing light absorption towards the shorter

299 wavelengths. Furthermore both the dynamical variation and the relative magnitude of the segregated
 300 AOC values are in good agreement with the results of former field experiments made using the
 301 Aethalometer model (Sandradewi et al., 2008a; Favez et al., 2010; Castanho and Artaxo 2001). On the
 302 other hand it is noteworthy that AOC_{wb} is actually not negligible at 1064nm but its averaged relative
 303 abundance in the total AOC at this wavelength was more than 20% throughout the campaign. Based
 304 on the deduced segregated AAE values the segregation of the AOC was made at the other two
 305 wavelengths too and the average relative abundance of AOC_{wb} in the total AOC was found to increase
 306 gradually toward the shorter wavelengths: 20.5%, 45.1%, 65.8% and 82.2% at 1064nm, 532nm,
 307 355nm and 266nm respectively.

308 The deduced segregated mass specific optical absorption values are highly plausible and are in
 309 good agreement with most of the similar data previously published in literature (Moosmüller et al.,
 310 2009; Petzold et al., 2004). Furthermore AAEff and AAEBwb values can also be derived from these
 311 values substituting sigmas in AOC in eq. 3 and 4. They were found to be 1.1 ± 0.2 and 2.62 ± 0.4
 312 respectively, which are in a reasonable agreement with values deduced by the extrapolation method,
 313 which further confirms the reliability of this approach.

314 It is important to emphasize that neither the AAE_{wb} nor the σ_{wb} values are representative to a
 315 specific wood type or burning condition but rather they correspond to a mixture of wood types and
 316 burning conditions as well as to ambient conditions i.e. most probably they can be used only for the
 317 analyzed measurement campaign under the actual local circumstances. The same applies for the traffic
 318 related segregated parameters, i.e. they also only represent local averages.

319 Finally as far as the segregated mass concentrations are concerned the calculated results show that,
 320 during the whole campaign, wood burning aerosol was dominant while traffic aerosol played only
 321 inferior role in CM(PM1). These findings are in line with other field experiments when the
 322 apportionment of wood burning emission was determined by Aethalometer model in urban or rural
 323 sites under wintry condition where dominantly wood burning contributed to residential heating.
 324 Furthermore, the average relative strength of wood burning to traffic aerosol was found to be around
 325 75% and the average cumulative mass of carbonaceous aerosol (wood burning plus traffic) about 50%
 326 of the total PM2.5 (measured nearby in the official monitoring station of Hungarian Air Quality
 327 Network (HAQN)) which are also very typical under such conditions (Flowers et al., 2010;
 328 Sandradewi et al., 2008a; Bressi et al., 2014; Fuller et al., 2014)

329

330 **6. Summary and conclusion**

331 A carbonaceous particulate selective source apportionment study was performed for ambient
 332 particulate matter in the city center of Szeged, Hungary where the dominance of traffic and wood
 333 burning aerosol has been experimentally demonstrated earlier (Utry et al., 2014). The proposed model
 334 is based on the parallel, in-situ measurement of optical absorption and size distribution. AAE_{ff} and

335 AAE_{wb} were deduced from the measured data using the defined correlation between the
 336 AOC(1064nm)/AOC(266nm) and N_{100}/N_{20} ratios. $\sigma_f(\lambda)$ and $\sigma_{wb}(\lambda)$ were determined with the help of
 337 the independently measured temporal mass concentrations in the PM1 mode. Furthermore, the
 338 proposed optical source apportionment is based on the assumption that the light absorbing fraction of
 339 PM is exclusively related to traffic and wood burning. This assumption is indirectly confirmed here by
 340 the fact that the measured size distribution is composed of two unimodal size distributions identified to
 341 correspond to traffic and wood burning aerosols. The method offers the possibility of replacing
 342 laborious chemical analysis with simple in-situ measurement of aerosol size distribution data. The
 343 results by the proposed novel optical absorption based source apportionment method prove its
 344 applicability whenever measurements are performed at an urban site where traffic and wood burning
 345 are the dominant carbonaceous sources of emission. Obviously, the effects caused by the activities of
 346 biogenic compounds or photochemistry as well as the changes in meteorological condition on the
 347 results of the extrapolation method should be further investigated in the future.

348

349 **Acknowledgement**

350

351 Financial support by the Hungarian Scientific Research Foundation (OTKA, project no. K101905) is
 352 gratefully acknowledged. The European Union and the European Social Fund have provided financial
 353 support to the project under the project no. TÁMOP FUTURICT 4.2.2.C-11/1/KONV-2012-0013 and
 354 GOP-1.1.1-11-2012-0114.

355

356 **References**

357

358 Ajtai, T., Filep, Á., Schnaiter, M., Linke, C., Vragel, C., Bozóki, Z., Szabó, G., Leisner, T. (2010a). A
 359 novel multi-wavelength photoacoustic spectrometer for the measurement of the UV-vis-NIR spectral
 360 absorption coefficient of atmospheric aerosols. *J Aerosol Sci* 41, 1020-1029.

361 Ajtai, T., Filep, Á., Kecskeméti, G., Hopp, B., Bozóki, Z., Szabó, G. (2010b). Wavelength dependent
 362 mass-specific optical absorption coefficients of laser generated coal aerosols determined from multi-
 363 wavelength photoacoustic measurements. *App Phys A* 103 (4), 1165-1172.

364 Ajtai, T., Filep, Á., Utry, N., Schnaiter, M., Linke, C., Bozóki, Z., Szabó, G., Leisner, T. (2011). Inter-
 365 comparison of optical absorption coefficients of atmospheric aerosols determined by a multi-
 366 wavelength photoacoustic spectrometer and an aethalometer under sub-urban wintry conditions. *J*
 367 *Aerosol Sci* 42, 859-866.

368 Andreae, M.O., Gelencsér, A., (2006) Black carbon or brown carbon? The nature of light-absorbing
 369 carbonaceous aerosol. *Atmospheric Chemistry and Physics* 6: 3131–3148.

370 Andreae, M.O., Merlet, P., (2001). Emission of trace gases and aerosols from biomass burning. *Global*
 371 *Biogeochemical Cycles* 15 (4), 955-966.

372 Bond, T. C. (2001) Spectral Dependence of Visible Light Absorption by Carbonaceous Particles
 373 Emitted from Coal Combustion, *Geophys. Res. Lett.*, 28(21), 4075–4078.

374 Bond, T.C., Covert, D.S., Kramlich, J.C., Larson, T.V., Charlson, R.J. (2002). Primary particle
 375 emissions from residential coal burning: optical properties and size distributions. *J Geophys Res:*
 376 *Atmos* (1984-2012) 107 (D21). ICC 9-1eICC 9-14.

377 Bond, T. C., Doherty, S. J., Fahey, D. W., Forster, P. M., Berntsen, T., DeAngelo, B. J., Flanner, M.
 378 Ghan, S., Kärcher, B., Koch, D., Kinne, S., Kondo, Y., Quinn, P. K., Sarofim, M. C., Schultz, M.
 379 Schulz, M., Venkataraman, C., Zhang, H., Zhang, S., Bellouin, N., Guttikunda, S. K., Hopke, P.
 380 K., Jacobson, M. Z., Kaiser, J. W., Klimont, Z., Lohmann, U., Schwarz, J. P., Shindell, D., Storelvmo,
 381 T., Warren, S. G., and Zender, C. S. (2013). Bounding the role of black carbon in the climate system: a
 382 scientific assessment, *J. Geophys. Res.-Athmos.*, 118, 1–173

383 Burtscher, H. (2005) Physical characterization of particulate emissions from diesel engines: a review. *J*
 384 *Aerosol Sci* 36 896 – 932

385 Bressi, M., Sciare, J., Ghersi, V., Mihalopoulos, N., Petit, J. E., Nicolas, J. B., Moukhtar, S., Rosso,
 386 A., Feron, A., Bonnaire, N., Poulakis, E., Theodosi, C. (2014) Sources and geographical origins of fine
 387 aerosols in Paris (France). *Atmos. Chem. Phys.*, 14: 8813–8839.

388 Castanho, A. D. A., Artaxo, P. (2001). Wintertime and summertime São Paulo aerosol source
 389 apportionment study. *Atmos. Environ.* Vol 35, Issue 29, 4889-4902.

390 Chakrabarty, R. K., Moosmüller, H., Chen, L.-W.A., Lewis, K., Arnott, W.P., Mazzoleni, C., Dubey,
 391 M.K., Wold, C.E., Hao, W.M., Kreidenweis, S.M. (2010). Brown carbon in tar balls from smoldering
 392 biomass combustion. *Atmospheric Chemistry and Physics* 10, 6363-6370.

393 Chow, J. C., John Watson, J. G, Crow, D., Lowenthal, D., H., Merrifield, T. (2001). Comparison of
 394 IMPROVE and NIOSH Carbon Measurements. *Aerosol Sci Tech*, 34:1, 23-34.

395 Dinar, E., Mentel, T. F., Rudich, Y (2006). The density of humic acids and humic like substances
 396 (HULIS) from fresh and aged wood burning and pollution aerosol particles. *Atmos. Chem. Phys.*, 6,
 397 5213–5224, 2006

398 Favez, O., Cachier, H., Sciare, J., Sarda-Esteve, R., Matignon, L. (2009). Evidence for a significant
 399 contribution of wood burning aerosols to PM2.5 during the winter season in Paris, France. *Atmos*
 400 *Environ* 43, 3640-3644.

401 Favez, O., El Haddad, I., Piot, C., Boréave, A., Abidi, E., Marchand, N., Jaffrezo, J.-L., Besombes, J.-
 402 L., Personnaz, M.-Z., Sciare, J., Wortham, H., George, C., D'Anna, B. (2010). Inter-comparison of
 403 source apportionment models for the estimation of wood burning aerosols during wintertime in an
 404 Alpine city (Grenoble, France). *Atmos Chem Phys* 10, 5295-5314.

405 Flowers, B.A., Dubey, M.K., Mazzoleni, C., Stone, E.A., Schauer, J.J., Kim, S.-W. (2010). Optical-
 406 chemical relationships for carbonaceous aerosols observed at Jeju Island, Korea with a 3-laser
 407 photoacoustic spectrometer. *Atmos. Chem. Phys.*, 10, 10387-10398.

408 Fuller, G.W., Tremper, A.H., Baker, T.D., Yttri, K.E., Butterfield, D. (2014) Contribution of wood
 409 burning to PM10 in London. *Atmos. Environ.*, 87: 87-94.

410 Harrison, R., M., Beddows, D., C., S., Jones, A., M., Calvo, A., Alves, C., Pio, C. (2013) An
 411 evaluation of some issues regarding the use of aethalometers to measure woodsmoke concentrations.
 412 Atmos. Environ., Vol. 80, 540-528.

413 Hedberg, E., Kristensson, A., Ohlsson, M., Johansson, C., Johansson, P.-A., Swietlicki, E., Vesely, V.,
 414 Wideqvist, U., Westerholm, R., 2002. Chemical and physical characterization of emissions from birch
 415 wood combustion in a wood stove. Atmos Environ 36, 4823e4837.

416 Kirchstetter, T. W. , Novakov, T., and Hobbs, P. (2004) Evidence that the spectral dependence of light
 417 absorption by aerosols is affected by organic carbon, J. Geophys. Res., 109, D21208,
 418 doi:10.1029/2004JD004999

419 Kleinman, L., I., Daum, P., H, Lee, Y., Senum, G., I., Springston, S., R., Wang, J., Berkowitz, C.,
 420 Hubbe, J., Zaveri, R., A., Brechtel, F., J., Jayne, J., Onasch, T., B., Worsnop, D. (2007) Aircraft
 421 observations of aerosol composition and ageing in New England and Mid-Atlantic States during the
 422 summer (2002). New England Air Quality Study field campaign. J Geophys. Res., Vol. 112, D09310,
 423 doi:10.1029/2006JD007786

424 Lack, D.A., Lovejoy, E.R., Baynard, T., & Pettersson, A. (2006). Aerosol absorption measurement
 425 using photoacoustic spectroscopy: Sensitivity, calibration and uncertainty developments. Aerosol Sci
 426 and Tech, 40, 697–708.

427 Lanz, V. A., Alfarra, M. R. ,U. Baltensperger, Buchmann, B., Hueglin, C. , Prévôt, A. S. H. (2007).
 428 Source apportionment of submicron organic aerosols at an urban site by factor analytical modelling of
 429 aerosol mass spectra. Atmos. Chem. Phys., 7, 1503-1522.

430 Lewis, K., Arnott, W.P., Moosmüller, H., Wold, C.E. (2008). Strong spectral variation of biomass
 431 smoke light absorption and single scattering Albedo observed with a novel dual-wavelength
 432 photoacoustic instrument. Journal of Geophysical Research 113 (d16), D16203.

433 McMurry, P., H., Wang, X., Park, K., Ehara, K. (2002) The Relationship between Mass and Mobility
 434 for Atmospheric Particles: A New Technique for Measuring Particle Density, Aerosol Science and
 435 Technology, 36:2, 227-238, DOI: 10.1080/027868202753504083

436 Moosmüller, H., Chakrabarty, R.K., Arnott, W.P. (2009). Aerosol light absorption and its
 437 measurement: a review. Journal of Quantitative Spectroscopy & Radiative Transfer 110, 844-878

438 Moosmüller, H., Chakrabarty, R.K., Ehlers, K.M., Arnott, W.P. (2011). Absorption Ångström
 439 coefficient, brown carbon, and aerosols: basic concepts, bulk matter, and spherical particles.
 440 Atmospheric Chemistry and Physics 11, 1217-1225.

441 Park, K., Kittelson, D. B., & McMurry, P. H. (2004). Structural properties of diesel exhaust particles
 442 measured by transmission electron microscopy (TEM): relationships to particle mass and
 443 mobility. Aerosol Science and Technology, 38, 881–889.

444 Penner, J.E., Hegg, D., & Leaitch, R. (2001). Unraveling the role of aerosols in climate
 445 change. Environmental Science and Technology, 35(15), 332A–340A

446 Rissler, J., Vestin, A., Swietlicki, E., Fisch, G., Zhou, J., Artaxo, P., Andreae, M.O. (2006). Size
 447 distribution and hygroscopic properties of aerosol particles from dryseason biomass burning in
 448 Amazonia. Atmospheric Chemistry and Physics 6, 471-491

449 Sandradewi, J., Prévôt, A.S.H., Szidat, S., Perron, N., Alfarra, M.R., Lanz, V.A., Weingartner, E., &
 450 Baltansperger, U. (2008a). Using aerosol light absorption measurements for the quantitative
 451 determination of wood burning and traffic emission contributions to particulate matter. *Environmental
 452 Science and Technology*, 42, 3316–3323

453 Sandradewi, J., Prévôt, A.S.H., Weingartner, E., Schmidhauser, R., Gysel, M., & Baltensperger, U.
 454 (2008b). A study of wood burning and traffic aerosols in an Alpine valley using a multi-wavelength
 455 Aethalometer. *Atmospheric Environment*, 42, 101–112.

456 Scaire, J., Oikonomou, K., Favez, O., Liakakou, E., Markaki, Z., Cachier H., Mihalopoulos, N. (2008)
 457 Long-term measurements of carbonaceous aerosols in the Eastern Mediterranean: evidence of long-
 458 range transport of biomass burning. *Atmos. Chem. Phys.*, 8, 5551-5563

459 Schnaiter, M., Horvath, H., Mohler, O., Naumann, K. H., Saathoff, H., and Schock, O. W. (2003).
 460 UV-VIS-NIR spectral optical properties of soot and soot-containing aerosols, *J. Aerosol Sci.*, 34,
 461 1421– 1444.

462 Schnaiter, M., Schmid, O., Petzold, A., Fritzsche, L., Klein, K. F., Andreae, M. O., Helas, G.,
 463 Thielmann, A., Gimmler, M., Möhler, O., Linke, C., Schurath, U. (2005) Measurement of
 464 Wavelength-Resolved Light Absorption by Aerosols Utilizing a UV-VIS Extinction Cell, *Aerosol
 465 Science and Technology*, 39:3, 249-260, DOI: 10.1080/027868290925958

466 Schneider, J., Weimer, S., Drewnick, F., Borrmann, S., Helas, G., Gwaze, P., Schmid, O., Andreae,
 467 M.O., Kirchner, U., 2005. Mass spectrometric analysis and aerodynamic properties of various types of
 468 combustion-related aerosol particles. *International Journal of Mass Spectrometry* 258 (1-3), 37-49.

469 Schwartz, S.E. (2004). Uncertainty requirements in radiative forcing of climate change. *Journal of the
 470 Air and Waste Management Association*, 54(11), 1351

471 Solomon, S., Qin, D., Manning, M., Chen, Z., Marquis, M., Averyt, K.B., Tignor, M., & Miller, H.L.
 472 (Eds.). (2007). *Contribution of Working Group I. To the Fourth Assessment Report of the
 473 Intergovernmental Panel on Climate Change*. Cambridge University Press: Cambridge, United
 474 Kingdom and New York, NY, USA.

475 Turpin, J., & Lim, H. (2001) Species Contributions to PM2.5 Mass Concentrations: Revisiting
 476 Common Assumptions for Estimating Organic Mass, *Aerosol Science and Technology*, 35:1, 602-610

477 Utry, N., Ajtai, T., Filep, Á., Pintér, M., Török, Z., Bozóki, Z., Szabó, G. (2014) Correlations between
 478 absorption Angstrom exponent (AAE) of wintertime ambient urban aerosol and its physical and
 479 chemical properties, *Atmospheric Environment* 91, 52-59.

480 Wehner, B., Wiedensohler, A. (2003). Long term measurements of submicrometer urban aerosols:
 481 statistical analysis for correlations with meteorological conditions and trace gases. *Atmospheric
 482 Chemistry and Physics* 3, 867-879.

- We introduce a new method for the real time source apportionment of atmospheric aerosol
- The method is deduced from a field measurement campaign
- The method requires the measurement of size distribution and optical absorption
- The applied instruments are a SMPS and a multi-wavelength photoacoustic absorption spectrometer